their findings, and at the same time rule out a similar type of structure for the products we obtained in the present study, we repeated their experiment and obtained a white crystalline product with UV absorption data and melting point identical with those reported by Wierzchowski and Shugar. To further test their structural assignment, we analyzed the compound by NMR. On the NMR time scale we would expect the product to appear to have the symmetrical structure shown in braces in Scheme II. The ^{1}H NMR spectrum recorded in acetonitrile-d_3 (TMS standard) showed a six-proton singlet at 2.18 ppm (2 CH_3), a broad two-proton singlet at 7.73 ppm (2 NH), and a fairly sharp one-proton resonance at 11.50 ppm (N··H··N). This supports their structural assignment. As Wierzchowski and Shugar point out, the simplest and most plausible route of formation of this compound proceeds through a C2–C5 Dewar intermediate. Although the intermediate Dewar structures for 2,6-dimethyl-4-aminopyrimidine and those we propose as intermediates in the reactions of cytosine derivatives are different, the presence of the 4-amino group common to both appears to allow facile decomposition of the Dewar structures to form open-chain nitriles.

Photoreaction of 2′-Deoxycytidine To Form VIa and VIb Is Insensitive to Oxygen and Is Not Photosensitized by Acetone. One piece of information of photochemical interest is the nature of the excited-state precursor(s) of the ureidoacrylonitriles. In particular, it is desirable to know whether excited singlet, triplet, and/or "hot" (highly vibrationally excited) ground states of the parent cytosines are involved in the photoreaction. We have studied the effect of oxygen quenching and acetone photosensitization on the reaction of 2′-deoxycytidine (VI) to form VIa and VIb, in order to gain information about the possible involvement of the triplet state of VI. Deoxygenation of either an aqueous or an acetonitrile solution of 2′-deoxycytidine (2 mM) and irradiation for 1 h at 254 nm showed no significant change in yield of formation of products VIa and VIb as compared to aerated samples, based on HPLC measurements. Furthermore, we did not observe reaction to produce VIa and VIb when VI was irradiated in the presence of 5% acetone at $\lambda > 300$ nm for 1 h. Both of these observations suggest that a triplet state is not involved; however, in drawing this conclusion, we have to make assumptions that the energy level for the triplet state of acetone is higher than that of 2′-deoxycytidine and that the rate constant of oxygen quenching is sufficiently large to inactivate the triplet state before the putative Dewar intermediate forms. The first assumption is probably valid; although the triplet energy of 2′-deoxycytidine is evidently not known, the triplet energy level of cytidine 5′-monophosphate lies below the triplet state of acetone.[32] The second assumption, however, is more questionable as the intramolecular rearrangement of the triplet state of VI to form a Dewar intermediate could be extremely fast.

Conclusions

We have reported here the isolation and characterization of a novel class of photoproducts produced when cytosine, 5-methylcytosine, and related compounds are irradiated with ultraviolet light, namely the 3-ureidoacrylonitriles. The simplest and most plausible mechanism for formation of these compounds involves the initial formation of the N3–C6 Dewar valence isomer, followed by rearrangement to the final product. In addition to their photochemical interest, these findings may be relevant to understanding the effects of ultraviolet radiation on DNA and, thus, could have significant photobiological importance.

Abbreviations

Key: TSP, 2-(trimethylsilyl)propionate-*2,2,3,3-d*$_4$; TMS, tetramethylsilane; HPLC, high-performance liquid chromatography; COSY, two-dimensional correlation spectroscopy; LSIMS, liquid secondary ion mass spectrometry; T.L.C., thin-layer chromatography.

Acknowledgment. Research support from the NIH (Grant GM 23526) is gratefully acknowledged. Also acknowledged is the Bio-organic, Biomedical Mass Spectrometry Resource (A. L. Burlingame, Director), supported by NIH Division of Research Resources Grant RR01614.

Supplementary Material Available: UV absorbance spectrum of compound VIA and 300-MHz ^{1}H NMR spectrum of Vb measured in acetonitrile-d_3 against TMS (2 pages). Ordering information is given on any current masthead page.

(32) Reference 3, Table I, p 239 and references therein.

Application of the Structural Correlation Method to Ring-Flip Processes in Benzophenones

Zvi Rappoport,*,† Silvio E. Biali,*,† and Menahem Kaftory*,‡

Contribution from the Department of Organic Chemistry, The Hebrew University of Jerusalem, Jerusalem 91904, Israel, and the Department of Chemistry, Technion—Israel Institute of Technology, Haifa 32000, Israel. *Received March 5, 1990*

Abstract: Thirty-eight crystallographically independent structures of thirty-two benzophenones were retrieved from the Cambridge Structural Data Base. All except one show an helical propeller conformation. The torsional angles of the two rings ϕ_1 and ϕ_2 were plotted one against the other in order to identify the threshold enantiomerization mechanism by applying the structural correlation method to the potential ring-flip processes. Molecular mechanics (MM) calculations on benzophenone gave the corresponding calculated potential energy surface. An excellent agreement with the calculated route for a one-ring flip was obtained from the conformational map of the crystallographic data, especially in benzophenones where the C=O bond is involved in intramolecular hydrogen bonding. The strong preference for this route is rationalized by the tendency to maximize the Ar—C=O conjugation interaction during the rotation. The structural correlation method can be used also to evaluate trends in the changes of the structural parameters, such as bond lengths and angles in approaching the rotational transition state. Similar trends are obtained from analysis of the X-ray data and from MM calculations on the one-ring flip of benzophenone.

Introduction

By using literature data we recently[1] applied the structural correlation method[2-4] to assess the most feasible ring flip routes in 1,1-diaryl- and 1,1,2-triarylvinyl systems.[1] Both the one- and the two-ring flips were found to be feasible for 1,1-diarylvinyl

† The Hebrew University of Jerusalem.
‡ Technion—Israel Institute of Technology.

(1) Kaftory, M.; Nugiel, D. A.; Biali, S. E.; Rappoport, Z. *J. Am. Chem. Soc.* **1989**, *111*, 8181.

0002-7863/90/1512-7742$02.50/0

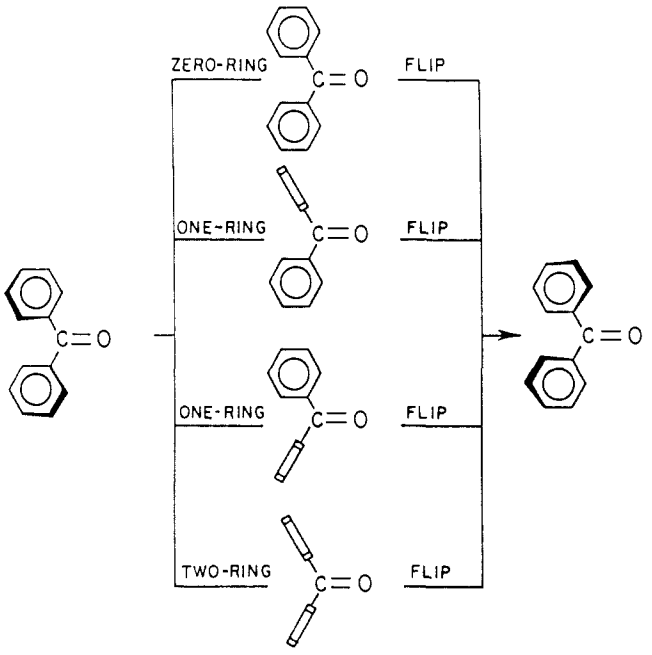

Figure 1. Idealized transition states for zero-, one- (β and β'), and two-ring flips in $Ar^1Ar^2C{=}O$. An open rectangle indicates a ring that is perpendicular to the C=C plane.

propellers, and molecular mechanics (MM) calculations indicated that the former is preferred in the parent 1,1-diphenylethylene (**1**). This analysis was in agreement with the experimentally found shift in the rotational mechanism of lowest activational energy (threshold mechanism) in 2,2-dimesityl-1-substituted-ethenols.[5]

$$\underset{\mathbf{1}}{Ph_2C{=}CH_2} \qquad \underset{\mathbf{2}}{Ph_2C{=}O}$$

The $Ar^1Ar^2C = X$ moiety is present in other families, e.g., where X = N or O. Of special interest are benzophenones (X = O) whose static and the dynamic stereochemistry was investigated by a wide variety of methods.[6] All methods agree that the preferred conformation is helical (propeller) (cf. Figure 1), but disagree on the values of the twist angles of the aryl rings.

Idealized transition states for the rotational routes leading to enantiomerization of helical benzophenone (**2**) are shown in Figure 1. When the rings rotate in concert (correlated rotation), both conrotatory and disrotatory routes are possible. In the conrotatory routes both rings are coplanar (zero-ring flip) or perpendicular (two-ring flip) with the $\diagdown\!\!>C{=}O$ plane in the idealized transition state. In the disrotatory one-ring flip, one ring is coplanar with, and the other perpendicular to, the C=O plane.

Benzophenones differ from 1,1-diarylethylenes in two important respects: (a) the higher conjugative $\pi(C{=}O)$-$\pi(Ar)$ interaction should be reflected in the ground-state conformation, and in the preferred rotational route around the =C—Ar bonds; (b) properly situated hydrogen-bond-donating substituents can form intramolecular hydrogen bonds which may affect these conformations and routes.

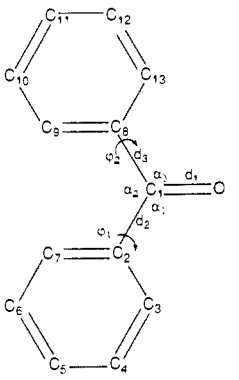

Figure 2. Labeling of bonds, bond angles, and torsional angles for benzophenone.

The barriers to conrotatory and disrotatory ring rotation in benzophenone were previously calculated by both MNDO and STO-3G methods.[6] Both methods show that the threshold rotational mechanism is the one-ring flip. MM calculations on the crowded 2,2',6,6'-tetramethylbenzophenone indicated, as in the case of **2**, that the one-ring flip mechanism is favored over the two-ring flip.[7]

Dynamic NMR data are mostly restricted to crowded benzophenones. The dynamic behavior of 2,4,6-triisopropylbenzophenone and its derivatives[8a,b] was analyzed in terms of a nonpropeller-preferred conformation, and uncorrelated rings rotation. For several benzophenones and their complexes, the disrotatory one-ring flip is the preferred rotational pathway.[8c]

In the present work we retrieved the crystallographically determined structures of benzophenones from the Cambridge Structural Database (CSD)[9] and used these data together with MM calculations to analyze the rotational behavior of benzophenones by the structural correlation method and to compare it with that of 1,1-diarylethylenes.[10,11] Aryl heteroaryl ketones or diheteroaryl ketones[12] have been excluded from our analysis.

Results and Discussion

The Diaryl Ketones Data Base. A search of the CSD[9] (1987 release) retrieved 65 benzophenones. For 19 of these, detailed information was not available or there were errors in the coordinates. Eleven structures with R values >0.10 (some belonging to the group above) were excluded from the analysis. This left 32 compounds with 38 crystallographically independent molecules,

(2) (a) Burgi, H.-B. *Angew. Chem., Int. Ed. Engl.* **1975**, *14*, 460. (b) Dunitz, J. D. *X-ray Analysis and the Structure of Organic Molecules*; Cornell University Press: Ithaca, NY, 1979. (c) Burgi, H.-B.; Dunitz, J. D. *Acc. Chem. Res.* **1983**, *16*, 153. (d) Murray-Rust, P.; Burgi, H. B.; Dunitz, J. D. *Acta Crystallogr.* **1979**, *A35*, 703.

(3) For applications of the Structural Correlation method see, for example: (a) Nachbar, R. B., Jr.; Johnson, C. A.; Mislow, K. *J. Org. Chem.* **1982**, *47*, 4829. (b) Jones, P. G.; Kirby, A. J. *J. Am. Chem. Soc.* **1984**, *106*, 6207. (c) Cosse-Barbi, A.; Dubois, J. E. *Ibid.* **1987**, *109*, 1503.

(4) The rotational mechanism of some triaryl systems has been derived from the analysis of crystal structures: Bye, E.; Schweizer, W. B.; Dunitz, J. D. *J. Am. Chem. Soc.* **1982**, *104*, 405. Clegg, W.; Lockart, J. C. *J. Chem. Soc., Perkin Trans. 2* **1987**, 1621.

(5) Biali, S. E.; Nugiel, D. A.; Rappoport, Z. *J. Am. Chem. Soc.* **1989**, *111*, 846.

(6) Abraham, R. J.; Haworth, I. S. *J. Chem. Soc., Perkin Trans. 2* **1988**, 1429 and references cited therein.

(7) Finocchiaro, P. *Gazz. Chim. Ital.* **1975**, *105*, 149.

(8) (a) Ito, Y.; Umehara, Y.; Nakamura, K.; Yamada, Y.; Matsuura, T. *J. Org. Chem.* **1981**, *46*, 4359. (b) Bonini, B. F.; Grossi, L.; Lunazzi, L.; Macciantelli, D. *Ibid.* **1986**, *51*, 517. (c) Weissensteiner, W.; Scharf, J.; Schlogl, K. *Ibid.* **1987**, *52*, 1210.

(9) For a description of the Cambridge Structural Database and its potential for mechanistic studies, see: (a) Allen, F. H.; Bellard, S.; Brice, M. D.; Cartwright, B. A.; Doubleday, A.; Higgs, H.; Hummelink, T.; Hummelink-Peters, B. G.; Kennard, O.; Motherwell, W. D. S.; Rogers, J. R.; Watson, D. G. *Acta Crystallogr., Sect. B.*, **1973**, *35*, 2331. (b) Allen, F. H.; Kennard, O.; Taylor, R. *Acc. Chem. Res.* **1983**, *16*, 146.

(10) (a) Part of the work was briefly described: Rappoport, Z.; Biali, S. E.; Kaftory, M. Sixth European Symposium on Organic Chemistry, (ESOC 6), Belgrade, Yugoslavia, September 10–15, 1989, Abst. B-0-009, p. 333. Kaftory, M.; Biali, S. E.; Rappoport, Z. 12 European Crystallographic Meeting, Moscow, USSR, August 20–29, 1989, Abs. p. 256. (b) We recently learned that Klebe reached a similar conclusion regarding the threshold enantiomerization route by using MNDO rather than MM calculations. We thank Dr. Klebe for sending us his figure which resembles our Figure 3A.

(11) An analogous case are triarylimines. However, the dihedral angles of the phenyl rings for the five $Ph_2C{=}NAr$ structures found in the CSD (Naqvi, R. R.; Wheatley, P. J. *J. Chem. Soc. A* **1970**, 2053. Jochims, J. C.; Lambrecth, J. L.; Burkert, U.; Szolnai, L.; Huthner, G. *Tetrahedron* **1984**, *40*, 893) are too similar for application of structural correlation analysis for identifying the ring-flip process.

(12) For papers dealing with conformational analysis of aryl heteroaryl ketones, see: (a) Benassi, R.; Folli, U.; Iarossi, D.; Scheretti, L.; Taddei, F. *J. Chem. Soc., Perkin Trans. 2* **1987**, 1443. (b) Benassi, R.; Folli, U.; Iarossi, D.; Scheretti, L.; Taddei, F.; Musatti, M.; Nardelli, M. *Ibid.* **1987**, 1443 and references therein.

Table I. Crystallographic Data for $Ar^1Ar^2C{=}O$

no.	Ar^1	Ar^2	ref code	group[a]	d_1 (C=O), Å	d_2, Å	d_3, Å	α_1, deg	α_2, deg	α_3, deg	ϕ_1, deg	ϕ_2, deg	ref
1	Ph	Ph	BPHENO10	S1	1.231	1.484	1.496	119.2	121.8	119.0	29.4	30.9	*b*
2	3-BrC_6H_4	3-BrC_6H_4	BRBEPH	S2	1.203	1.503	1.503	119.2	121.6	119.2	26.9	26.9	*c*
3	4-ClC_6H_4	4-ClC_6H_4	CBENPH	S1	1.220	1.535	1.535	119.2	121.6	119.2	27.8	27.8	*d*
3a			CBENPH01	S1	1.210	1.481	1.481	119.6	120.9	119.6	27.8	27.8	*e*
4	4-IC_6H_4	4-IC_6H_4	ZZZOVY01	S1	1.222	1.494	1.494	119.3	121.3	119.3	26.9	26.9	*f*
5a	4-$O_2NC_6H_4$	4-$O_2NC_6H_4$	NOPHKN	S1	1.220	1.482	1.510	120.5	121.0	118.5	21.5	36.5	*g*
5b				S1	1.216	1.500	1.506	120.4	119.8	119.9	27.6	34.3	*g*
6a	2-Me-1-Np[h]	2-Me-1-Np[h]	MNPKET	S2	1.218	1.496	1.497	120.7	119.3	120.0	49.8	56.8	*i*
6b				S2	1.222	1.501	1.505	121.1	118.7	120.3	48.6	49.6	*i*
7	4-$N_2NC_6H_4$	4-$H_2NC_6H_4$	AMBZPH	S1	1.240	1.473	1.481	120.8	119.5	119.7	25.9	35.8	*j*
8a	4-$C_6H_4C_6H_4COPh$-4	Ph	BZOBPH	A1	1.223	1.477	1.478	119.7	120.4	119.9	26.5	30.3	*k*
8b				A1	1.231	1.474	1.498	119.3	122.8	117.9	27.6	29.6	*k*
9	Ph	A[l]	CIDRAI	A2	1.215	1.489	1.494	120.0	120.0	120.0	16.8	40.9	*m*
10a	Ph	2,7-Me_2-8-PhCO-1-Np[h]	BOMNPH	A,O	1.226	1.470	1.501	121.2	118.8	119.8	14.3	83.3	*n*
10b				A2,O	1.187	1.486	1.502	122.3	117.8	119.9	10.8	77.9	*n*
11	2-Np[h]	2,4,6-i-$Pr_3C_6H_2$	BAZZIL10	A2,O	1.215	1.485	1.511	123.2	118.6	118.2	17.9	84.1	*o*
12	Ph	2-*t*-BuC_6H_4	DECWAJ01	A2,O	1.214	1.491	1.503	120.9	118.8	120.2	8.0	70.6	*p*
13	Ph	5-PhCO-1-Np[h]	DBONAP	A2,O	1.218	1.490	1.504	120.8	119.7	119.4	20.2	57.6	*q*
14	2-O_2N-4-$MeO_2CC_6H_3$	Mes[r]	MCNBZP10	A2,O	1.210	1.500	1.502	119.0	118.5	122.5	38.7	51.6	*s*
15	2-$PhCH_2N{=}C(Ph)C_6H_4$	Ph	BULHIZ	A2,O	1.223	1.501	1.488	118.1	122.1	119.8	32.4	40.3	*t*
16	3-i-Pr-4-$MeOC_6H_3$	2,6-I_2-4-$MeO_2CC_6H_2$	DIPMOB10	A3,O	1.250	1.448	1.524	123.5	119.2	117.2	5.3	84.2	*u*
17a	2,4-$(HO)_2C_6H_3$	2,4-$(HO)_2C_6H_3$	BADVIL10	S2,O,H	1.259	1.458	1.464	119.5	122.3	118.3	18.6	28.3	*v*
17b				S2,O,H	1.269	1.450	1.455	118.7	123.6	117.7	16.4	32.6	*v*
18	Ph	4-EtO-8-HO-1-Np[h]	BYEXNO	A2,O	1.223	1.489	1.503	119.6	120.6	119.3	15.1	76.3	*w*
19	3-Br-2-HOC_6H_3	2-$HOOCC_6H_4$	BROHBZ	A3,O,H	1.238	1.509	1.478	120.2	120.9	118.5	−6.8	83.9	*x*
20	2-$H_2NC_6H_4$	Ph	DEMBAY	A2,O,H	1.231	1.464	1.492	122.7	118.8	118.5	17.8	56.4	*y*
21	Ph	2-HO-3-AcO-5-MeC_6H_2	BAGPAA	A2,O	1.217	1.477	1.505	121.1	119.6	119.2	28.8	50.9	*z*
22	2-$H_2NC_6H_4$	2-$HOOCC_6H_4$	AMBZAC	A3,O,H	1.243	1.447	1.514	122.7	120.1	117.1	7.4	65.3	*aa*
23	2-$HOOCC_6H_4$	3-Cl-4-HOC_6H_5	QQQHDS10	A3,O	1.212	1.482	1.504	124.9	116.0	118.7	18.5	79.7	*bb*
24	2-HO-3-Cl-6-$MeOC_6H_2$	B[cc]	CHBCOU	A3,O,H	1.228	1.476	1.491	119.4	122.2	118.4	20.6	50.6	*dd*
25	2,4-$(HO)_2C_6H_3$	Ph	DHXBZP10	A2,O,H	1.253	1.453	1.489	120.4	122.1	117.5	7.6	46.4	*ee*
26	2-HO-4-$MeOC_6H_3$	Ph	HMXBZP	A2,O,H	1.255	1.447	1.500	121.0	122.9	116.1	10.5	42.7	*ff*
27	2-HO-4-$MeOC_6H_3$	4-ClC_6H_4	HMXCBP10	A2,O,H	1.247	1.474	1.490	120.3	121.8	117.9	8.7	42.4	*gg*
28	2-HO-4-ClC_6H_3	2-$HOOCC_6H_4$	CLOHBZ	A3,O,H	1.240	1.463	1.517	122.0	120.6	117.1	4.9	87.6	*hh*
29	2-HO-5-ClC_6H_5	2-$HOOCC_6H_4$	CLHBZL	A3,O,H	1.228	1.481	1.486	120.8	120.0	118.9	5.1	78.1	*ii*
30	2,6-$(HO)_2$-4-$MeOC_6H_2$	3-HO-2-$(CHCH{=}CMe_2)C_6H_3$	CUDRAN	A2,O,H	1.249	1.447	1.498	120.8	122.2	117.0	7.8	74.4	*jj*
31	C[kk]	Ph	COPKIB	A2,O,H	1.240	1.469	1.505	121.0	122.0	117.1	22.9	51.6	*ll*
32	2-HOC_6H_4	D[mm]	SALBZF	A3,O,H	1.247	1.445	1.499	122.0	121.4	116.6	4.6	58.6	*nn*

[a] Abbreviations are as follows: S, Symmetrical; AS, apparently symmetrical; A, asymmetric; O, ortho substituted; H, Hydrogen bonded. [b] Fleischer, E. B.; Sung, N.; Hawkinson, S. *J. Phys. Chem.* **1968**, *72*, 4311. [c] Pattabhi, V.; Venkatesan, K. *J. Cryst. Mol. Struct.* **1973**, *3*, 25. [d] Shields, K. G.; Kennard, C. H. L. *J. Chem. Soc., Perkin Trans. 2* **1977**, 463. [e] Granger, M. M.; Coillot, M. F. *Acta Crystallogr., Sect. C* **1985**, *C41*, 542. [f] Van der Velden, G. P. M.; Noordik, J. H. *J. Cryst. Mol. Struct.* **1979**, *9*, 283. [g] Chiari, G.; Traylor, H. C. R.; Fronczek, F. R.; Newkome, G. R. *Acta Crystallogr., Sect. B* **1980**, *B36*, 2488. [h] Np = naphthyl. [i] Fink, R.; Van der Helm, D. *Cryst. Struct. Commun.* **1980**, *9*, 97. [j] Van der Velden, G. P. M.; Noordik, J. H. *J. Cryst. Mol. Struct.* **1980**, *10*, 83. [k] Loesburg, H. M.; Noordik, J. H. *Cryst. Struct. Commun.* **1979**, *8*, 377. [l] See structure below. [m] Mairesse, G.; Boivin, J. C.; Thomas, D. J.; Bermann, M. C.; Bonte, J. P.; Lesieur, D. *Acta Crystallogr., Sect. C* **1984**, *C40*, 1019. [n] Gore, P. H.; Henrick, K. *Ibid. Sect. B* **1980**, *B36*, 2462. [o] Takemoto, Y.; Fukuyama, K.; Tsukihara, T.; Katsube, Y.; Ito, Y.; Matsuura, T. *Rep. Fac. Eng. Tottori Univ.* **1983**, *14*, 148. [p] Wagner, P. J.; Giri, B. P.; Scaiano, J. C.; Ward, D. L.; Gabe, E.; Lee, F. L. *J. Am. Chem. Soc.* **1985**, *107*, 5483. [q] Noordik, J. H. *Cryst. Struct. Commun.* **1978**, *7*, 663. [r] Mes = mesityl (2,4,6-$Me_3C_6H_2$). [s] Van der Hejden, S. P. N.; Chadler, W. D.; Robertson, B. E. *Can. J. Chem.* **1975**, *53*, 2127. [t] Ruiz-Valero, C.; Monge, A.; Gutiérrez-Puebla, E. *Acta Crystallogr., Sect. C* **1983**, *C39*, 795. [u] Cody, V.; Cheung, E.; Jorgensen, E. C. *Acta Crystallogr., Sect. B* **1982**, *B38*, 2270. [v] Schlemper, E. O. *Ibid.* **1982**, *B38*, 554. [w] Deppisch, B.; Nigam, G. D.; Bernhard, E.; Neidlein, R. *Ibid. B*, **1978**, *B34*, 3840. [x] Skrzat, Z.; Konitz, A. *Pol. J. Chem.* **1980**, *54*, 1029. [y] Antolini, L.; Vezzosi, I. M.; Battaglia, L. P.; Corradi, A. B. *J. Chem. Soc., Perkin Trans. 2* **1985**, 237. [z] Ray, T.; Sen Gupta, S. P. *Cryst. Struct. Commun.* **1981**, *10*, 1123. [aa] Skrzat, Z.; Roszak, A. *Acta Crystallogr., Sect. B* **1981**, *B37*, 770. [bb] Skrzat, Z. *Pol. J. Chem.* **1980**, *54*, 795. [cc] See structure below. [dd] Gorst-Allman, C. P.; Nolte, M. J.; Steyn, P. S. *S. Afr. J. Chem.* **1978**, *31*, 143. [ee] Liebich, B. W. *Acta Crystallogr., Sect. B* **1979**, *B35*, 1186. [ff] Liebich, B. W.; Parthé, E. *Ibid.* **1974**, *B30*, 2522. [gg] Liebich, B. W. *Ibid.* **1976**, *B32*, 431. [hh] Skrzat, Z. *Acta Crystallogr. Sect. B* **1980**, *B36*, 2812. [ii] Skrzat, Z. *Ibid.* **1980**, *B36*, 3201 [jj] Otterson, T.; Vance, B.; Doorenbos, N. J.; Chang, B.-L.; El-Feraly, F. S. *Acta Chem. Scand., Sect. B* **1977**, *B31*, 434. [kk] See structure below. [ll] Ishiguro, K.; Yamaki, M.; Takagi, S.; Yamagata, Y.; Tomita, K. E. *J. Chem. Soc., Chem. Commun.* **1985**, *26*. [mm] See structure below. [nn] Bergman, J.; Egestad, B.; Rajapaksa, D. *Acta Chem. Scand., Ser. B* **1979**, *33*, 405.

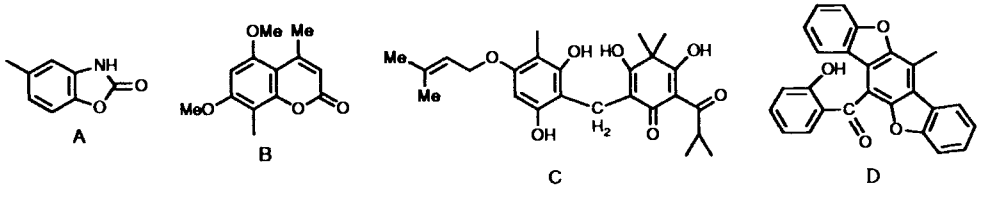

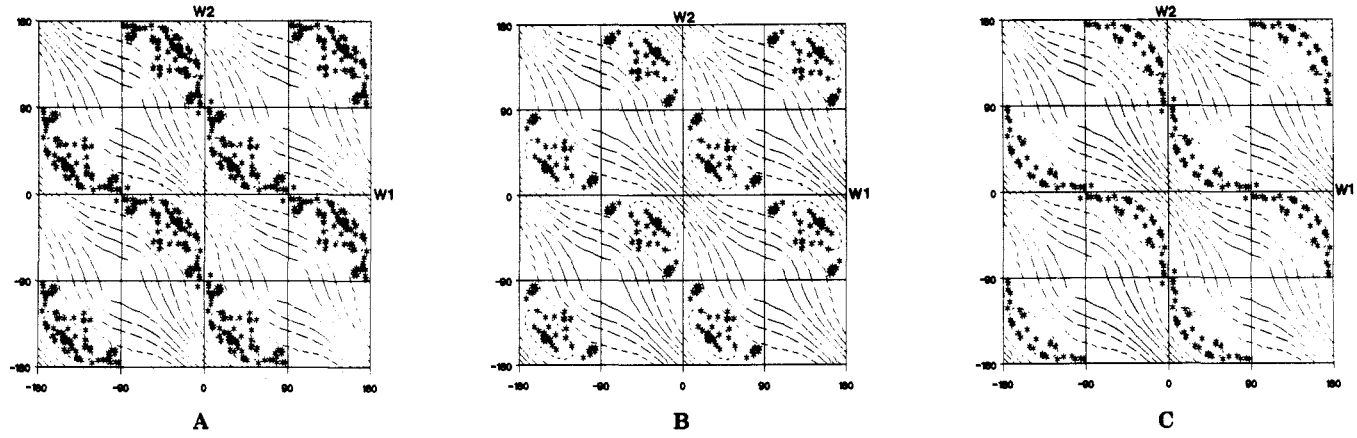

Figure 3. Conformational map (ω_1 vs ω_2) for benzophenones. ω_1 and ω_2 denote the angles equivalent to ϕ_1 and ϕ_2 which are generated by the symmetry of the benzophenone skeleton. The contours are calculated equipotential energy regions for **2** and are spaced by 1.35 kcal mol^{-1}. The points are for ϕ_1, ϕ_2 of $Ar^1Ar^2C{=}O$ from Table I. Parts of the figure are as follows: (A) all compounds, (B) non-hydrogen-bonded compounds, (C) hydrogen-bonded compounds.

Table II. Calculated Energies and Structural Parameters for the Ground State and Rotational Transition States of Benzophenone[a]

parameter[a]	ground state	transition state for *n*-ring flip			
		zero-ring	one-ring	two-ring	C_{2v}[b]
relative energy	0	7.5	1.4	6.8	8.7
C(1)-O	1.23	1.23	1.23	1.22	1.24
α_1	120.2	117.4	123.0	122.7	115.1
α_2	119.6	125.3	117.3	114.7	129.8
α_3	120.2	117.4	119.6	122.7	115.1
C(1)-C(2)-C(3)	119.1	118.0	121.4	119.5	116.7
C(1)-C(2)-C(7)	121.5	123.8	119.4	119.7	127.5
C(1)-C(8)-C(13)	119.0	118.0	119.5	119.5	116.7
C(1)-C(8)-C(9)	121.5	123.8	119.6	119.6	127.5
O-C(1)-C(2)-C(7)	150	162[c]	180	90	180[c]
O-C(1)-C(8)-C(9)	149	162[d]	90	90	180[c]

[a] Energies are in kcal mol^{-1}, bond lengths in Å, angles in degrees. [b] Planar structure of C_{2v} symmetry (see text). [c] O-C(1)-C(2)-C(7)) = 0°. [d] O-C(1)-C(8)-C(13) = 0°.

and their structures, bond lengths and angles and torsional angles (cf. Figure 2 for labeling) are given in Table I. The compounds belong to several subgroups, but in practice, semiquantitative differences were found only between hydrogen-bonded and non-hydrogen-bonded systems.

Molecular Mechanics Calculations. The potential energy map of benzophenone (**2**) as a function of the torsional angles of the rings was calculated by Baraldi et al. using the CINDO method.[13] Parts of the potential energy surface were recently calculated by the MNDO and the ab initio (STO-3G) methods with partial geometry optimization.[6] We recalculated the whole potential energy map using Allinger's molecular mechanics program, MM2(85).[14] The torsional angle of one of the rings was driven from 0° to 180°, and that of the other from 0° to 90° in 10° increments.

The results are plotted in a contour map in Figure 3. Calculated energies and selected structural parameters are given in Table II. The calculated geometries of the different transition states are shown in Figure 4. As shown graphically in Figure 3, the lower energy region corresponds to a propeller conformation with $\phi_1 = \phi_2 = 30°$ in agreement with the crystallographically determined (X-ray) values (29.4°; 30.9°).[15] The calculated threshold rotational route corresponds to a disrotatory motion of the rings (a one-ring flip route) with a barrier of 1.4 kcal mol^{-1},

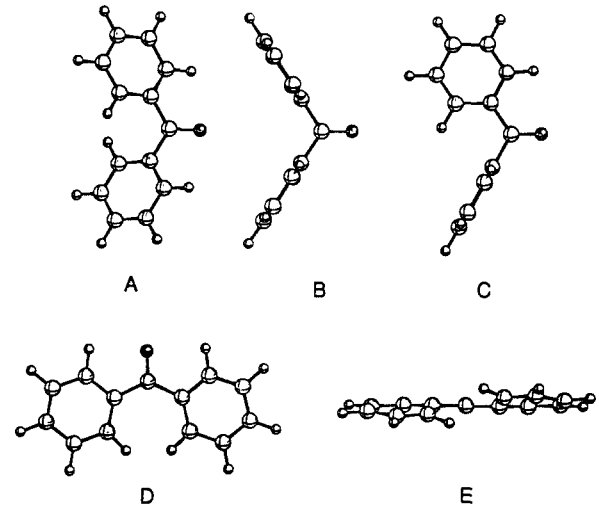

Figure 4. Calculated (MM2(85)) conformations of the lower energy form (A) and the transition states (viewed from a normal to the C>C=O plane) for the two-ring flip (B), the one-ring flip (C), and zero-ring flip (D), also viewed along the C=O bond (E) of benzophenone.

whereas the two conrotatory routes (zero- and two-ring flips) have higher barriers (7.5 and 6.8 kcal mol^{-1}, respectively). The calculated transition state of the zero-ring flip adopts an helical conformation of C_2 symmetry (cf. Figure 4). The deviation from planarity is reflected by the O-C(1)-C(2)-C(7) and the O-C(1)-C(8)-C(9) torsional angles of 162°. A planar C_{2v} structure lies 1.2 kcal mol^{-1} above the C_2 structure.

A comparison between the calculated potential map of **1** and **2** is of interest. The torsional angles of the ground-state conformation of **2** (30°) are smaller than those calculated for **1** (40°), in agreement with the lower steric requirements of the oxygen of **2** compared with CH_2 in **1** and the larger conjugation energy of **2**. The calculated energy difference (MM2(85)) between the one- and two-ring flip routes is larger for **2** (5.4 kcal mol^{-1}) than for **1** (1.8 kcal mol^{-1}). This suggests that the one-ring–two-ring flip dichotomy in thresholds mechanisms which exist for derivatives of **1**, is absent for derivatives of **2**. Consequently, these systems should undergo helicity reversal exclusively via a one-ring flip. Baraldi et al. found similar trends in their calculations, although the increase in the energy gap between the barriers for the two-ring and the one-ring flip routes are less pronounced (1.1 kcal mol^{-1} for **1**, 2.6 kcal mol^{-1} for **2**).[13] Our calculated barriers of **2** resemble the calculated barriers for the one- and two-ring flip processes using STO-3G calculations (1.2 and 6 kcal mol^{-1}). The calculated barrier for the zero-ring flip process is lower in **2** than in **1** (7.5 and 12.9 kcal mol^{-1}, respectively), probably due to a higher Ph—C=O as compared to a Ph—C=C conjugation energy. The

(13) Baraldi, I.; Gallinela, E.; Momicchioli, F. *J. Chem. Phys.* **1986**, *83*, 653.

(14) Allinger, N. L. MM2(85). *QCPE Bull.* **1985**, *5*, 139. See also Sprague, J. T.; Tai, J. C.; Yuh, Y. H.; Allinger, N. L. *J. Comput. Chem.* **1987**, *8*, 581.

(15) Fleischer, E. B.; Sung, N.; Hawkinson, S. *J. Phys. Chem.* **1968**, *72*, 4311. Similar results but with a higher *R* value were reported by Lobanova, G. M. *Kristallografiya* **1968**, *13*, 984.

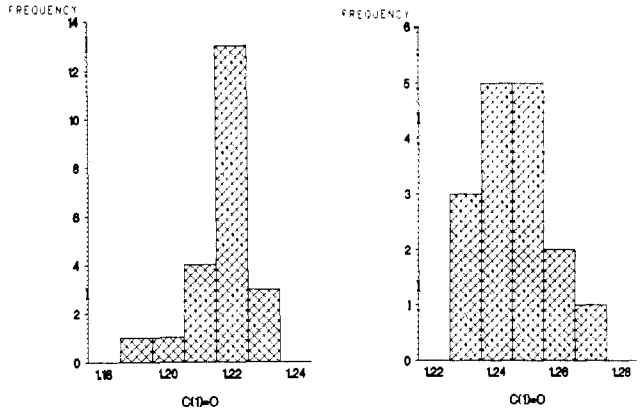

Figure 5. Histogram of frequency of appearance vs C=O bond length in non-hydrogen-bonded and hydrogen-bonded benzophenones (A and B, respectively).

deviation of 18° from planarity of the rings in the transition state for the zero-ring flip of **2** is less pronounced than the corresponding deviation of 26° for **1**, in agreement with the expected larger loss of conjugation energy in **2**.

Application of the Structural Correlation Method. In the calculated conformational map of benzophenone (Figure 3 parts A–C) the contours are drawn 1.35 kcal mol^{-1} apart. Superimposed on the contour map of Figure 3A are the experimental points for all the data given in Table I. In Figure 3B,C these are subdivided into the compounds with no intramolecular hydrogen bonds involving the C=O group and ortho-substituents and intramolecularly hydrogen-bonded diaryl ketones, respectively.

The clear outcome from Figure 3 is that all compounds are spread, nearly evenly, along the (90°,0°);(0°,90°) diagonal, whereas the (0°,0°);(90°,90°) diagonal is not represented except for points common to both diagonals. Also shown is the absence of points except one, in the square defined by the (0° → −90°);(0° → 90°) axes, indicating that 37 out of the 38 structures have a propeller structure, i.e., the two rings are twisted in the same sense. The exception is item 19 in Table I where one ring is nearly perpendicular to the C=O plane (83.9°) and the other is nearly coplanar, but twisted in the opposite sense (−6.8°). This compound deviates consistently in correlations involving bond lengths and angles. The hydrogen-bonded derivatives follow the minimum energy path much more closely (Figure 3C) than the other derivatives, which cluster in several regions, including around the calculated (30°,30°) minimum (Figure 3B).

The application of structural correlation method is straightforward. The preferred minimum energy path for the correlated rotation of the two rings of **2** is a one-ring flip. No indication for the two-ring or the zero-ring flip processes, (i.e., presence of points near the extremes of the (0°,0°);(90°,90°) diagonal), is observed. Consequently, both the MM calculations and the application of the structural correlation method lead to the same conclusion.

Intramolecular Hydrogen Bonding in *o*-Hydroxydiaryl Ketones. In the structure correlations, we separated intramolecularly ortho-substituted hydrogen-bonded systems from non-hydrogen-bonded ones. Compounds clearly identified as having intramolecular O—H···O=C hydrogen bonds are those with O···O non-bonded distances of 2.50–2.72 Å. The presence of hydrogen bonding requires spatial proximity of the hydrogen-bonded groups. This may also be reflected in other structural properties, such as alternate changes in the bond lengths to atoms involved in the bonding, as shown in Gilli's work on hydrogen bonds in enols of β-diketones.[16] For the hydrogen-bonded *o*-hydroxybenzophenones (**3**), the C=O bond length should be elongated as compared with non-hydrogen-bonded benzophenones whereas the C—O and the C_1—Ar bonds should shrink.

(16) Gilli, G.; Bellucci, F.; Ferreti, V.; Bertolasi, V. *J. Am. Chem. Soc.* **1989**, *111*, 1023.

Table III. Observed Correlations between Bond Lengths, Bond Angles, and Torsional Angles for Benzophenones and Corresponding Calculated Relationships for the One-Ring Flip of Benzophenone

correlation equation	type[a]
$d_1 = 1.230(8)-0.00003(14)\phi_2$	exp, A
$d_1 = 1.221(7)-0.00004(12)\phi_2$	exp, NHB
$d_1 = 1.269(9)-0.00044(15)\phi_2$	exp, HB
$d_2 = 1.484(1) + 0.00025(3)\phi_1$	cal
$d_2 = 1.463(6) + 0.00080(25)\phi_1$	exp, A
$d_2 = 1.458(5) + 0.00058(11)\phi_1$	exp, NHB
$d_2 = 1.486(4) + 0.00026(9)\phi_1$	exp, HB
$d_3 = 1.4752(19) + 0.00048(3)\phi_2$	cal
$d_3 = 1.485(7) + 0.00024(12)\phi_2$	exp, A
$d_3 = 1.495(7) + 0.00011(12)\phi_2$	exp, NHB
$d_3 = 1.460(12) + 0.00057(20)\phi_2$	exp, HB
$d_2 = 1.495(1) - 0.00013(1)\phi_2$	cal
$d_2 = 1.490(9) - 0.00021(16)\phi_2$	exp, A
$d_2 = 1.505(3) - 0.00026(8)\phi_2$	exp, NHB
$d_2 = 1.493(6) - 0.00044(12)\phi_2$	exp, HB
$d_3 = 1.5164(19) - 0.00092(12)\phi_1$	cal
$d_3 = 1.497(5) - 0.00005(2)\phi_1$	exp, A
$d_3 = 1.507(7) - 0.00026(25)\phi_1$	exp, NHB
$d_3 = 1.495(8) - 0.00026(59)\phi_1$	exp, HB
$\Delta d = -0.002(1) - 0.00041(2)\Delta\phi$	cal
$\Delta d = 0.0074(51) + 0.00034(12)\Delta\phi$	exp, A
$\Delta d = 0.0030(37) + 0.00043(10)\Delta\phi$	exp, NHB
$\Delta d = 0.0276(161) + 0.000007(303)\Delta\phi$	exp, HB
$\alpha_2 = 122.77(64) - 0.043(11)\phi_2$	exp, A
$\alpha_2 = 122.96(60) - 0.060(11)\phi_2$	exp, NHB
$\alpha_2 = 132.28(1.01) - 0.036(17)\phi_2$	exp, HB
$\alpha_1 = 123.05(16) - 0.093(10)\phi_1$	cal
$\alpha_1 = 118.16(49) + 0.048(9)\phi_2$	exp, A
$\alpha_1 = 117.63(51) + 0.061(9)\phi_2$	exp, NHB
$\alpha_1 = 119.291(1.02) + 0.025(17)\phi_2$	exp, HB
$\alpha_2 = 124.74(46) - 0.084(6)(\phi_1 + \phi_2)$	cal
$\alpha_2 = 125.20(82) - 0.06505(1107)(\phi_1 + \phi_2)$	exp, A
$\alpha_2 = 124.83(1.00) - 0.065(13)(\phi_1 + \phi_2)$	exp, NHB
$\alpha_2 = 125.08(1.43) - 0.056(20)(\phi_1 + \phi_2)$	exp, HB
$d_1 = 1.0964(313) + 0.0011(3)\alpha_2$	cal
$d_1 = 0.480(170) + 0.00621(141)\alpha_2$	exp, A
$d_1 = 0.883(138) + 0.00279(115)\alpha_2$	exp, NHB
$d_1 = 0.662(206) + 0.00481(170)\alpha_2$	exp, HB
$d_2 = 2.078(278) - 0.00496(230)\alpha_1$	exp, A
$d_2 = 1.839(243) - 0.00289(201)\alpha_1$	exp, NHB
$d_2 = 1.958(411) - 0.00409(340)\alpha_1$	exp, HB
$\Delta d = -0.056(5) + 0.0098(19)\Delta\alpha$	cal
$\Delta d = 0.004(3) + 0.00788(102)\Delta\alpha$	exp, A
$\Delta d = 0.006(3) + 0.00619(112)\Delta\alpha$	exp, NHB
$\Delta d = -0.010(8) + 0.01225(228)\Delta\alpha$	exp, HB

[a] exp = correlation of crystallographic data; cal = calculation for the one-ring flip of **2**; A = all benzophenones; HB = only hydrogen-bonded benzophenones; NHB = only non-hydrogen-bonded benzophenones.

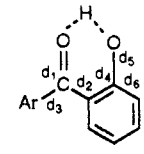

3

The lengthening of the C=O bonds which are involved in hydrogen bonding is clearly demonstrated in the comparison of the histograms shown in Figure 5 parts A and B. In non-hydrogen-bonded compounds the C(1)=O bond lengths are concentrated at ca. 1.22 Å (Figure 5A). In the hydrogen bonded systems, the most frequent bond lengths are 1.24–1.25 Å (Figure 5B) with an average of 1.245 Å, a value larger than any value shown in Figure 5A.

The change in the C—O bond length is unexpected. In enols of β-diketones this bond shrinks appreciably with intramolecular hydrogen bonding.[16] The C—O bond lengths in hydrogen-bonded benzophenones are indeed mostly shorter than the standard C—O bond length value of 1.362 Å.[17] However, a plot of the C=O

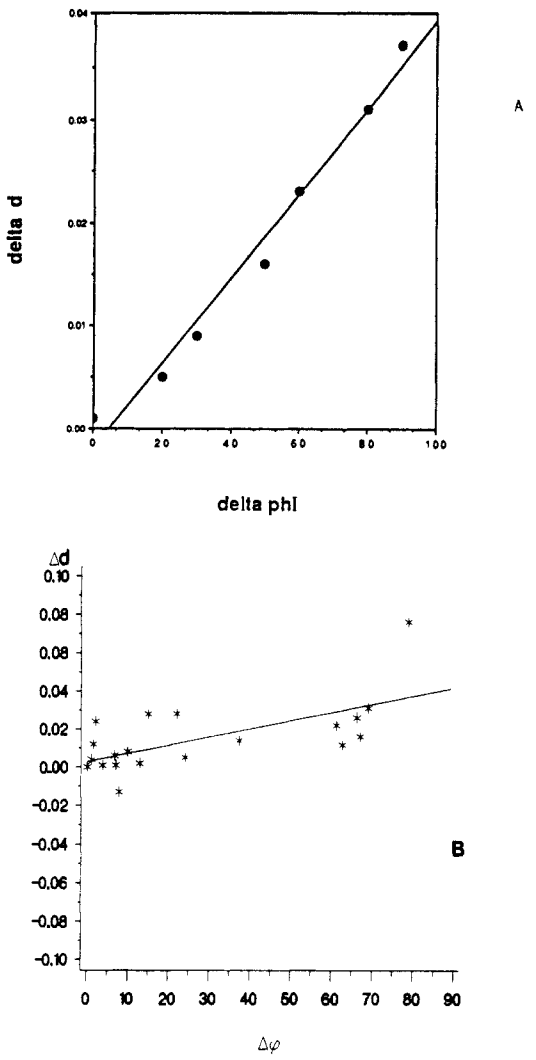

Figure 6. Δd vs $\Delta\phi$ plots. Parts of the figure are as follows: (A) calculated for the one-ring flip of benzophenone, and (B) experimental points for non-hydrogen-bonded benzophenones.

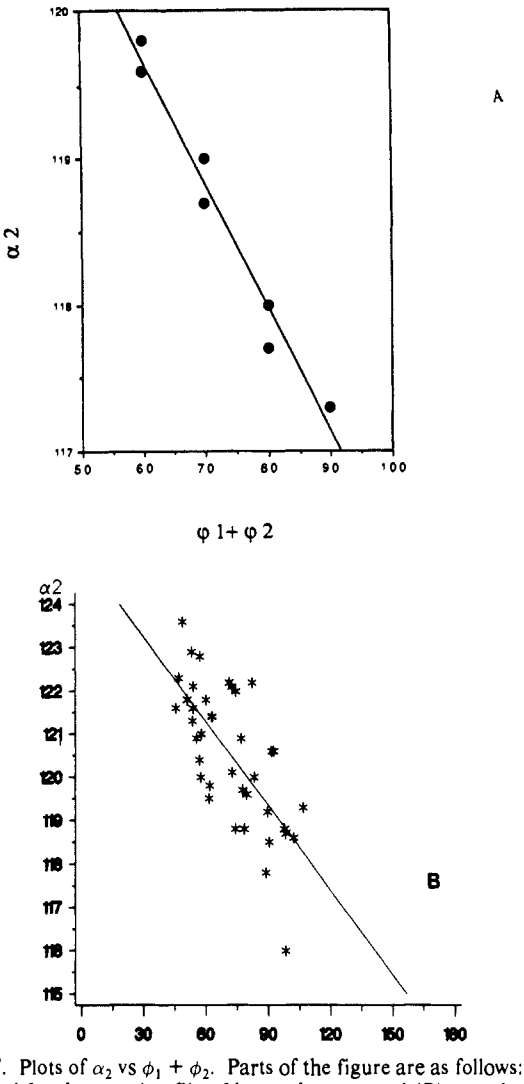

Figure 7. Plots of α_2 vs $\phi_1 + \phi_2$. Parts of the figure are as follows: (A) calculated for the one-ring flip of benzophenone, and (B) experimental points for all benzophenones.

(d_1) vs the C—O (d_5) bond length (supplementary material Figure S1) shows a regular increase, and the slope of 1.1 of the least-squares regression (eq 1) shows that the mutual changes in both

$$d(\text{C=O}) = 1.1(\mathbf{1})d(\text{C—O}) - 0.2(\mathbf{2}) \qquad (1)$$

bond lengths are in the same direction to approximately the same extent. Consequently, if the C=O bond length is taken as an indication of the extent of hydrogen bonding then the C—O bond length increases rather than decreases with the formation of hydrogen bonding. The reason for this is not yet clear.

For aryl groups not involved in hydrogen bonding the range of the C_1—Ar bond lengths is the normal sp^2–sp^2 bond length of 1.47–1.52 Å with the most frequent value at 1.50 Å. An exception (1.535 Å) is for 4,4′-dichlorobenzophenone. When the aryl group is involved in the intramolecular hydrogen bonding the C_1—Ar bond is shorter (1.45–1.48 Å), with the most frequent value at 1.45 Å. An exception is again item 19. The histograms are in supplementary material Figure S2. Supplementary material Figure S3 shows the difference between the two aromatic bond lengths to the C(OH) carbon in **3**. Bond d_6 anti to d_2 is much shorter (1.365–1.405 Å) than bond d_4 geminal to d_2 (1.40–1.43 Å).

Correlations Involving Bond and Torsional Angles and Bond Lengths. In addition to the change in ϕ_1 and ϕ_2 as the rotation progresses along the threshold mechanism, the bond lengths and angles should also change. Hence, correlations between them may be as valuable in delineating the threshold process. For example, for steric reasons, the angle α_2 is expected to open in the zero-ring flip and presumably to shrink in the two-ring flip. For conjugation reason, both d_2 and d_3 are expected to decrease during the zero-ring flip, to increase during the two-ring flip and to change in opposite directions in the one-ring flip. Since the one-ring flip for **2** is well established (Figure 3) we calculated the changes in bond lengths and angles for this route and correlated them with one another. The same crystallographic parameters were then correlated for all compounds together and for hydrogen-bonded and non-hydrogen-bonded benzophenones separately. In general, the calculated and the experimental (crystallographic) plots show the same trend although the scatter in the experimental plots is usually larger. Consequently, the structural correlation treatment can be applied with reasonable confidence, to evaluate the *direction* of the changes in bond lengths and angles during the threshold rotational process.

Due to the $\cos^2\phi$ dependence of the extent of the Ar—CO overlap, the conjugation decreases along the one-ring flip route. ϕ_2 was chosen as the torsional angle of the flipping ring and therefore we predict that the C=O bond (d_1) and the bond to the nonflipping ring (d_2) should shrink while the bond to the flipping ring (d_3) should elongate with the progress of the rotation. Intuitively, for steric reasons α_1 should increase and α_2 and α_3 should decrease along the rotation. Consequently, plots of d_1, d_2, α_2, or α_3 vs ϕ_2, or of d_3 or α_1 vs ϕ_1, and of d_2 vs α_1, and of d_3 vs α_2 should show a descending trend, whereas plots of d_3 or α_3 vs ϕ_2, of d_1, d_2, α_2, or α_3 vs ϕ_1, and of d_1 vs α_2, d_2 vs α_3, and of d_3 vs α_1 should show a parallel increase in both parameters. Since

(17) (a) Allen, F. H.; Kennard, O.; Watson, D. G.; Brammer, L.; Orphen, A. G.; Taylor, R. *J. Chem. Soc., Perkin Trans. 2* **1987**, S1. (b) It is expected that the value will be shorter in phenols due to conjugation with the ring, but intermolecular hydrogen bonds will affect these values.

the changes are small, the trends will be amplified in plots of $\Delta d(= d_3 - d_2)$, $\Delta\phi(= \phi_2 - \phi_1)$, and $\Delta\alpha(= \alpha_1 - \alpha_3)$ vs the α's, d's, and ϕ's. The changes will presumably be higher for the α_1 vs ϕ_2 plot. $\Delta\alpha(= \alpha_1 - \alpha_3)$ vs $\Delta\phi$ or vs Δd plots should also show ascending trends.

Since ϕ_2 changes more than ϕ_1 along the rotation we expect better correlations vs ϕ_2 than vs ϕ_1. Moreover, severe scatter in the correlations due to errors in the measured values are expected since the overall changes in bond lengths and angles along the rotation are not very large. Several plots are given in supplementary material Figures S4-S30. For convenience they were treated as linear even when the scatter was appreciable, and the slope of many correlations are given in Table III.

Calculated and experimental d_1 vs ϕ_2 plots (Figure S4) show a descending trend, d_1 vs ϕ_1 plots show large scatter, d_2 vs ϕ_1 and d_3 vs ϕ_2 (Figure S5) plots show an ascending trend. Calculated and experimental d_2 vs ϕ_2 and d_3 vs ϕ_1 show negative trends (Figures S6-S15). The derived $\Delta d(=d_3 - d_2)$ vs $\Delta\phi(\phi_2 - \phi_1)$ correlation (Figure 6) demonstrates the scatter observed in most of the experimental correlations.

Experimental plots of angle α_2 vs ϕ_1 show a large scatter. The calculated plot shows an ascending trend. The complementary α_2 vs ϕ_2 plots (Figures S16-S18), of α_1 vs ϕ_1 (Figures S19-S22) and (with a large scatter) for α_3 vs ϕ_2 plots, show descending trends. Ascending trends with appreciable scatter were observed for the calculated α_3 vs ϕ_1, α_1 vs ϕ_2, and $\Delta\alpha$ vs $\Delta\phi$ plots. Scatters were also observed in the α_2 vs $\Delta\phi$ plots which show descending trend (Figures S23-S25). The sum $\phi_1 + \phi_2$ for **2** generally increases during the one-ring flip process. The expected decrease of α_2 vs $\phi_1 + \phi_2$ is displayed in the calculated and experimental plots (Figures 7 and S26). For few non-hydrogen-bonded compounds $\phi_1 + \phi_2 > 90°$ in the ground state, but the overall trend parallels the calculated plots.

In the bond length vs bond angle correlations (Figures S27-S29) d_1 vs α_2 plots are reasonably linear with a positive slope. d_2 vs α_1 and d_3 vs α_3 plots show descending trend with scatter. Calculated d_2 vs α_3 and d_3 vs α_1 plots show severe scatter with ascending trend. The experimental ascending Δd vs $\Delta\alpha$ plot for non-hydrogen-bonded benzophenones (Figure S30) is one of the best correlations.

Consequently, correlations exist between various structural parameters of the benzophenones and are frequently amplified in the hydrogen-bonded systems. Since the one-ring flip is the favored rotational route, the trends indicated by both the experimental correlations and the MM calculations predict the changes in the structural parameters accompanying rotations of the rings. For example, from Figures S4B, S5, S15, and S22, d_1 for the hydrogen-bonded systems decreases by 0.02 Å, d_3 increases by 0.015 Å for non-hydrogen-bonded systems, α_2 decreases by ca. 3° and α_1 increases by ca. 3.5°, during the rotation. Both calculated and observed Δd vs $\Delta\phi$ plots (Figure 6) indicate an increase of 0.04 Å in Δd from the equilibrium value to the value in the rotational transition state, where $\Delta\phi \simeq 90°$.

Conclusions

In contrast with the 1,1-diarylethylenes which show a one-ring/two-ring flip dichotomy of rotational pathways, helical benzophenones undergo a helicity reversal process exclusively via a one-ring flip process. This is ascribed to the larger Ar—C=X conjugation energy for X = O (benzophenones) than in X = CR_2 (1,1-diarylethylenes). The structural correlation method is used for tracing the preferred rotational mechanism, and for grossly evaluating the structural parameters of the transition state. A complementary analysis of X-ray data and calculation can be used to derive reliably these structural parameters.

Acknowledgment. We are grateful to the United States-Israel Binational Science Foundation (BSF), Jerusalem, Israel, and The Bat-Sheva de Rothschild Fund for support of this work.

Registry No. 2, 119-61-9.

Supplementary Material Available: Figures S1-S30 of correlations between various bond lengths, bond angles, and torsional angles for benzophenones and calculations of changes in these parameters for the one-ring flip of **2** (24 pages). Ordering information is given on any current masthead page.

Proton Transfers among Oxygen and Nitrogen Acids and Bases in DMSO Solution

Calvin D. Ritchie* and Shanzheng Lu

Contribution from the Department of Chemistry, State University of New York at Buffalo, Buffalo, New York 14214. *Received May 14, 1990*

Abstract: Rate constants for the proton-transfer reactions between conjugate acids and bases of several amines, phenols, carboxylic acids, and the solvated proton in DMSO-d_6 at 20 °C have been determined by the use of NMR line-shape analysis. Equilibrium constants for the same reactions are obtained from the pK_a's of the acids in dimethyl sulfoxide, some of which have been reported in earlier work and the rest obtained in the present work by use of Bordwell's indicator techniques. All of the reactions have rate constants considerably below expected diffusion-controlled limits for the proton transfers in the thermodynamically favorable direction, and several of the reactions, including the identity reactions of carboxylic acids, have kinetic deuterium isotope effects, k_H/k_D, between 0.8 and 1.3. For reactions of *N*,*N*-dimethylbenzylammonium ion with several phenoxides, carboxylates, and solvent, the rate constants for transfers in the unfavorable directions show a reasonable Brønsted correlation with $\beta \approx 1$ and a reasonably constant reverse rate constant of $\approx 3 \times 10^6$ M^{-1} s^{-1}. The data clearly indicate that the proton-transfer step is not rate-limiting in these reactions. Most likely, desolvation is involved in the rate-limiting steps, but the rate constants are not simple functions of acidities as might have been expected if hydrogen bonding of acid to solvent were the major factor involved in the solvation. Other factors, particularly dispersion interactions of solvent with solutes, are discussed. We suggest that the formation of an acid-base complex with proper orientation to allow contact between the proton and the basic site is rate-determining and involves desolvation along with detailed steric interactions of the acid-base pair.

Eigen's classic studies[1] established the fact that proton transfers between electronegative atoms (specifically, O, N, and F) in aqueous solution frequently occur with diffusion-limited rates in the thermodynamically favorable direction. In the three-step

0002-7863/90/1512-7748$02.50/0